Plasmon spectrum in low-dimensional electron systems over insulating cryogenic films: Screening, quantum degeneracy, and multisubband effects

Sviatoslav S. Sokolov
Departamento de Física, Universidade Federal de São Carlos, 13565-905, São Carlos, São Paulo, Brazil and B. I. Verkin Institute for Low Temperature Physics and Engineering, National Academy of Sciences of Ukraine, 61103 Kharkov, Ukraine

Nelson Studart
Departamento de Física, Universidade Federal de São Carlos, 13565-905, São Carlos, São Paulo, Brazil
(Received 18 November 2002; revised manuscript received 29 July 2003; published 7 November 2003)

Plasmon modes in low-dimensional (quasi-one- and quasi-two-) electron systems floating over a cryogenic (liquid helium among others) film covering a solid substrate are calculated. Screening effects on the electron-electron interaction due to the substrate are taken into account and the plasmon spectrum is evaluated in the random-phase approximation. The spectrum consists of longitudinal and transverse branches whose frequencies depend on the film thickness and the dielectric constant of the substrate. For a metal substrate the gapless longitudinal mode has a dispersion quite different from that for the bulk case. The transverse plasma mode is optical like with the gap close to the spectroscopic intersubband frequency.

DOI: 10.1103/PhysRevB.68.195403 PACS number(s): 73.21.−b, 73.63.−b, 67.70.+n

I. INTRODUCTION

Electrons in surface states induced by the image potential form a remarkable system confined to two dimensions that has been used to study a rich variety of physical phenomena. The electronic system floats over a substrate which exhibits a short-range repulsion and a negative work function. The most extensive studies have been made for the case of superfluid helium, but other interesting insulating media such as solid hydrogen and neon have been considered and other substrates with a negative work function are also possible. There exist several types of image-potential-induced states at the surface of metals but they decay rapidly in bulk states.[1]

Surface electrons (SE's) have been mainly investigated above the smooth surface of bulk liquid helium because of the quite small density of impurities (vapor atoms) at low temperatures and the weak scattering by surface excitations (ripplons). For $T>1$ K the SE scattering by atoms of the helium vapor predominates whereas the interaction with ripplons is responsible for dynamic properties at lower temperatures down to 0.1 K where the influence of scatterers becomes negligible. This circumstance makes SE a unique tool for studying collective phenomena in the low-dimensional electron system (LDES) nearly decoupled from scatterers.[2] However, an electrohydrodynamic instability of the surface restricts the accessible range of electron densities to $n_s \lesssim 10^9 \mathrm{cm}^{-2}$.[3,4] At these densities, the 2D Fermi energy $E_F = \pi\hbar^2 n_s/m \simeq 3\times 10^{-2}$ K for $n_s = 10^9$ cm^{-2}. Then this LDES behaves like a nondegenerate quasi-two-dimensional (Q2D) system down to 10^{-2} K.[1]

The situation is quite different when the electrons are deposited on a helium film of thickness d located over a solid substrate with dielectric constant $\varepsilon_s > \varepsilon$, where ε is the dielectric constant of helium.[5] The reasons are twofold. First, the range of electron densities attainable can be increased significantly because the van der Waals attraction of the helium by the substrate is quite strong and stabilizes the charged liquid surface at higher densities.[6,7] Second, the screening of the Coulomb interaction by the image forces in the substrate reduces the potential energy necessary to crystallize the system and thereby prevents the formation of the Wigner crystal. In this sense, the quantum regime ($T<E_F$) can be achieved on a helium film supported by a substrate with large dielectric constant. Densities of the order of 10^{11}–10^{12} cm^{-2} have been reported.[8–11]

The possibility of the existence of an itinerant phase for SE's on a helium film at very low temperature[12] motivates the study of the collective modes of the LDES whose density can be continuously varied to reach both degenerate and nondegenerate regimes. In the present work we calculate the collective behavior of the multisubband LDES over a cryogenic film. First we study the plasmon spectra for the quasi-two-dimensional electron system (Q2DES). The longitudinal plasmon mode for the screened interaction when only the lowest subband is occupied has been calculated in the nondegenerate regime within the random-phase approximation[13] (RPA) and within the Singwi-Tosi-Sjölander-Land self-consistent field approximation[14] (SCFA), and also in both approximations in the degenerate regime.[15] Now, we use the many-body formalism for the multisubband itinerant Q2DES to evaluate the dispersion laws for both longitudinal and transverse plasmons for arbitrary ε_s. This allows us to reach both strong ($\varepsilon_s \gg 1$) and weak ($\varepsilon_s \gtrsim 1$) screening limits.

The results obtained are rather general and can be applied to the LDES on a film of one medium at a semi-infinite substrate of another one. However, we emphasize the case of superfluid helium mainly because its surface smoothness, the possibility of the LDES reaching both nondegenerate and degenerate regimes and different screening limits, and experimental realization.

One should say that the study of the properties of SE's over a helium film is indeed a difficult experimental task due to the influence of substrate inhomogeneities which produce

other scattering processes due to interface roughness,[16] static charges trapped by defects, suppression of the film thickness due to the electrostatic pressure, and others. Furthermore the electron-ripplon scattering itself is modified considerably in comparison with the bulk case.[17] One hopes that experimental progress in sample preparation with smooth surfaces should be made for studying the LDES over helium films. In this connection theoretical investigations are timely.

We also calculate the plasma dispersion relation of the multisubband Q1DES over a liquid helium film which has been realized in channels filled with liquid helium.[18–20] The Q1DES plasma properties over bulk helium have been investigated in the itinerant phase[21] as well in the Wigner solid regime.[22] As far as we know, the formation of the nondegenerate Q1DES has been observed only on superfluid helium.

II. PLASMON SPECTRA FOR THE Q2DES

The many-body approach to the multisubband Q2DES is based on a dielectric function tensor depending on 2D wave number q and frequency ω:

$$\epsilon_{nn'mm'}(q,\omega)=\delta_{nm}\delta_{n'm'}-v_{nn'mm'}(q)\Pi_{mm'}(q,\omega). \quad (1)$$

Here $\Pi_{mm'}(q,\omega)$ is the screened density-density response function with δ_{nm} being the Kronecker symbol. The matrix elements of the Fourier-transformed Coulomb potential averaged over the electron wave functions $\chi_n(z)$ of subbands with indices n, n', m, and m' (equal to 1,2,3,...) $v_{nn'mm'}(q)$ are given by[2,23,24]

$$v_{nn'mm'}(q)=\int_0^\infty dz\int_0^\infty dz'\,\chi_n(z)\chi_{n'}(z)\times v(q)\chi_m(z')\chi_{m'}(z'), \quad (2)$$

where $v(q)$ is the bare electron-electron interaction and z is along the perpendicular direction to the electron layer. The electron motion is restricted to $z>0$ due to the approximately infinite potential barrier at the liquid-vapor boundary at $z=0$.

The spectrum of collective modes for the multisubband system can be found by the condition of the vanishing of the determinant of the dielectric matrix given in Eq. (1), i.e.,

$$\det|\epsilon_{nn'mm'}(q,\omega)|=0, \quad (3)$$

which cannot be solved analytically for an arbitrary number of subbands leading to an intricate equation for coupled inter subband and intrasubband plasmon modes.[24] In order to obtain an approximate solution of Eq. (3) one should analyze both the response functions $\Pi_{mm'}(q,\omega)$ and matrix elements $v_{nn'mm'}(q)$.

The response functions are evaluated within the RPA. Even though the RPA works well only for weakly interacting systems, previous studies for the Q2DES many-body properties beyond the RPA have shown that the excitation spectrum does not change appreciably.[14,15,25,26] In the RPA, the screened density-density response function, appearing in Eq. (1), is taken as the noninteracting response function, which for the multisubband system is given by[23]

$$\Pi^0_{nn'}(q,\omega)=\sum_{\mathbf{k},s}\frac{f_0(E_\mathbf{k}+\Delta_n)-f_0(E_{\mathbf{k+q}}+\Delta_{n'})}{\hbar\omega+E_\mathbf{k}+\Delta_n-E_{\mathbf{k+q}}-\Delta_{n'}+i\eta}, \quad (4)$$

where $E_\mathbf{k}=\hbar^2k^2/2m$, $\mathbf{k}$ is the 2D electron wave vector, Δ_n is the energy of the nth subband, η is a infinitesimal positive, and s is the spin index. For nondegenerate Q2DES, $\Pi^0_{nn'}(q,\omega)$ depends on the Boltzmann distribution function $f_0(E_\mathbf{k}+\Delta_n)=\exp[-(E_\mathbf{k}+\Delta_n)/T]$ normalized by the condition $\Sigma_{n,\mathbf{k},s}f_0(E_\mathbf{k}+\Delta_n)=N$ where N is the particle number. As was shown[2] the response function can be calculated exactly in this case for arbitrary values of q, n, and n'. For small q, one can simplify significantly the real part of the response functions in the range of frequencies satisfying the condition $|\omega|,|\omega\pm\omega_{21}|\gg\hbar qk_T/m+\hbar q^2/2m$ where $k_T=\sqrt{2mT}/\hbar$ is the thermal wave number and $\omega_{21}=(\Delta_2-\Delta_1)/\hbar$. Note that the imaginary part of the response function is exponentially small in comparison with the real part in that frequency interval.

The response function $\Pi^0_{nn'}(q,\omega)$ for the quantum Q2DES with $f_0(E_\mathbf{k}+\Delta_n)=[\exp(E_\mathbf{k}+\Delta_n-\mu)/T+1]^{-1}$ where μ is the chemical potential, can also be evaluated exactly[15,27] for $n=n'$. For $n\neq n'$, we find that for $q\to0$ it is simpler to calculate the response function directly from Eq. (4) for $T\ll E_F$ in the limit of $|\omega|,|\omega\pm\omega_{21}|\gg\hbar qk_F/m+\hbar q^2/2m$.[28] Now the Fermi wave number $k_F=\sqrt{2\pi n_s}$ replaces k_T. Note that the imaginary part of the response function should be taken to be zero in this approximation.

From the structure of $f_0(E_\mathbf{k}+\Delta_n)$ in both nondegenerate and degenerate regimes one concludes that, due to the exponential dependence of $f_0(E_\mathbf{k}+\Delta_n)$ on Δ_n/T, the contribution of $f_0(E_\mathbf{k}+\Delta_n)$ and $f_0(E_{\mathbf{k+q}}+\Delta_{n'})$ to Eq. (4) becomes negligible for $n,n'\geqslant2$, in comparison with that of n or $n'=1$ when $T\ll\Delta_2-\Delta_1$. In the absence of the electric field $E_\perp$ which pushes the SE's against the helium surface, one has $\Delta_2-\Delta_1\simeq6$ K and the shift increases significantly for $E_\perp\neq0$.[2,17] As a result, for $T<1$ K, the occupation of the $n=2$ subband is negligible because the probability of SE's escaping from the $n=1$ subband is proportional to $\exp[-(\Delta_2-\Delta_1)/T]$. Furthermore, for $E_\perp\neq0$, the difference between the subband energies n' and n increases by increasing $|n'-n|$. Furthermore, film effects do contribute to a large effective holding field acting on the SE's. In such a condition one disregards $\Pi_{nn'}(q,\omega)$ with $n,n'\geqslant2$ in Eq. (3) and obtains the following dispersion equation:

$$1-v_{1111}(q)\Pi^{(0)}_{11}(q,\omega)-v_{1212}(q)[\Pi^{(0)}_{12}(q,\omega)+\Pi^{(0)}_{21}(q,\omega)]+[v_{1111}(q)v_{1212}(q)-v^2_{1112}(q)]\times[\Pi^{(0)}_{12}(q,\omega)+\Pi^{(0)}_{21}(q,\omega)]\Pi^{(0)}_{11}(q,\omega)=0, \quad (5)$$

where the real parts of the response functions can be written in the long-wavelength limit as

$$\mathrm{Re}\,\Pi^0_{11}(q,\omega)=\frac{Nq^2}{m\omega^2}\left(1+\frac{3\tilde{E}q^2}{m\omega^2}\right) \quad (6)$$

and

$$\mathrm{Re}[\Pi^0_{12}(q,\omega)+\Pi^0_{21}(q,\omega)] = \frac{2N\omega_{21}}{\hbar(\omega^2-\omega_{21}^2)}\left[1+\frac{(\omega_{21}^2+3\omega^2)\tilde{E}q^2}{m(\omega^2-\omega_{21}^2)} + \frac{(\omega_{21}^2+\omega^2)\hbar q^2}{2m\omega_{21}(\omega^2-\omega_{21}^2)}\right], \tag{7}$$

where $\tilde{E}=T(E_F)$ for the nondegenerate (degenerate) case.

The next approximation to Eq. (5) is based on the structure of matrix elements $v_{1111}(q)$, $v_{1212}(q)$, and $v_{1112}(q)$. In a previous work[2] $v_{nn'mm'}(q)$ were evaluated for SE's over bulk helium. For SE's on a helium film the electron-electron interaction is much more complicated. To calculate it, we solve Poisson's equation for the electrostatic potential $\varphi\{\mathbf{r}',z'\}$ from an electron at $\{\mathbf{r},z\}$ where $z>0$ and the helium film is located at $-d<z'<0$. Using standard methods,[29] we find that

$$\varphi_{\mathbf{q}}(z',z)=\frac{2\pi e}{Sq}\{[e^{-q|z-z'|}+F_1(qd)e^{-q|z+z'|}]\Theta(z') +[F_2(qd)e^{-q|z-z'|}+F_3(qd)e^{q|z-z'|}]\Theta(-z') \times\Theta(z'+d)+2F_4(qd)e^{-q|z-z'|}\Theta(-z'-d)\}, \tag{8}$$

where $\Theta(z)$ is the step function and S is the area occupied by electrons. The functions $F_i(qd)$ which appear in Eq. (8) are $F_1(x)=[\varepsilon_s-\varepsilon^2-\varepsilon(\varepsilon_s-1)\coth(x)]/f(x)$, $F_2(x)=g(x)(\varepsilon_s+\varepsilon)e^x$, $F_3(x)=-g(x)(\varepsilon_s-\varepsilon)e^{-x-2qz}$, and $F_4(x)=\varepsilon g(x)e^x$ with $f(x)=\varepsilon_s+\varepsilon^2+\varepsilon(\varepsilon_s+1)\coth x$ and $g(x)=[f(x)\sinh x]^{-1}$. The Fourier transform of the Coulomb potential is obviously written as

$$v(q)=\frac{2\pi e^2}{Sq}[e^{-q|z-z'|}+F_1(qd)e^{-q|z+z'|}] \tag{9}$$

for $z'>0$. Note that for $z=z'=0$, the Eq. (9) reproduces the expressions for the Fourier-transformed potential for the electron pair located at $z=0$.[13–15] For $d\to\infty$, $F_1(x)=(1-\varepsilon)/(1+\varepsilon)$ and Eq. (9) coincides with the well-known expression $v(q)=2\pi e^{*2}e^{-q|z'-z|}/Sq$, where $e^{*2}=2e^2/(1+\varepsilon)$, for SE's over bulk helium if we take into account that $\varepsilon=1.057\simeq 1$.[2,23]

In order to calculate $v_{nn'mm'}(q)$ using Eq. (2) we need the subband wave functions $\chi_i(z)$ of the potential in the z direction given by[17]

$$V(z)=-\frac{Qe^2}{4z}-Q_1e^2\sum_{n=1}^{\infty}\frac{\lambda^{n-1}}{z+nd}+eE_\perp z, \tag{10}$$

where $Q=(\varepsilon-1)/(\varepsilon+1)$, $Q_1=\varepsilon(\varepsilon_s-\varepsilon)/[(1+\varepsilon)^2(\varepsilon_s+\varepsilon)]$, $\lambda=(\varepsilon-1)(\varepsilon_s-\varepsilon)/[(\varepsilon+1)(\varepsilon_s+\varepsilon)]$, and the third term appears in Eq. (10) for $E_\perp\neq 0$. The solid substrate is located at $z\leqslant -d$. The first and second terms of Eq. (10) correspond to the image potential felt by the electron at $z>0$ in the vapor phase. Equation (10) can be derived by calculating the inverse Fourier transform $v(\mathbf{r}',z')$ of Eq. (9) and defining the image force acting on the electron located in the point $\{\mathbf{r},z\}$ as $f_{im}=-[\nabla v(\mathbf{r}',z')]|_{\mathbf{r}'=\mathbf{r},z'=z}$. Only $(f_{im})_z=-\partial V(z)/\partial z$ does exist, where the potential energy $V(z)$ coincides with the first two terms of Eq. (10).[30]

As is known an analytical solution of the Schrödinger equation for the potential given by Eq. (10) is obtained only for $E_\perp=Q_1=0$ or $Q_0=Q_1=0$.[17] In the two-subband model, $\chi_1(z)$ and $\chi_2(z)$ can be determined by the variational method with variational parameters γ_1 and γ_2. Trial wave functions were proposed as[31]

$$\chi_1(z)=2\gamma_1^{3/2}z\exp(-\gamma_1 z) \tag{11}$$

and

$$\chi_2(z)=\frac{2\sqrt{3}\gamma_2^{5/2}z}{(\gamma_1^2-\gamma_1\gamma_2+\gamma_2^2)^{1/2}}\left[1-\left(\frac{\gamma_1+\gamma_2}{3}\right)z\right]\exp(-\gamma_2 z). \tag{12}$$

The variational procedure was described in Ref. 2 for the bulk case ($d\to\infty$). Here we generalize the method for finite d adding the energies

$$\Delta_1^{(d)}=-Qe^2\gamma_1[1-2\gamma_1 d-4(\gamma_1 d)^2 \times\exp(2\gamma_1 d)\mathrm{Ei}(-2\gamma_1 d)] \tag{13}$$

and

$$\Delta_2^{(d)}=-\frac{Qe^2\gamma_2}{2\{\gamma_1^2-\gamma_1\gamma_2+\gamma_2^2\}}\left\{\gamma_1^2-2\gamma_1\gamma_2-3\gamma_2^2-\frac{2}{3}(\gamma_2 d) \times(\gamma_1+\gamma_2)^2+\frac{2}{3}\gamma_2^2[3+(\gamma_1+\gamma_2)d]^2 \times[1-2\gamma_2 d-4(\gamma_2 d)^2\exp(2\gamma_2 d)\mathrm{Ei}(-2\gamma_2 d)]\right\} \tag{14}$$

to the energies Δ_1 and Δ_2 given by Eqs. (8c) and (8d) of Ref. 2. Here $\mathrm{Ei}(x)$ is the integral exponential. $\Delta_1^{(d)}$ and $\Delta_2^{(d)}$ are due to the SE polarization coming from the solid substrate. Obtaining the subband energies for finite d one determines the variational parameters in a straightforward way.[32,33]

Using the trial wave functions given by Eqs. (11) and (12) one can calculate the matrix elements exactly for arbitrary values of q. The calculation is, however, rather cumbersome. For this reason we restrict ourselves to the long-wavelength limit $q\ll\gamma_1,\gamma_2,d^{-1}$ where the subband matrix elements of the Coulomb potential are given by

$$v_{1111}(q)=\frac{4\pi e^2}{Sq}\left\{\Phi(qd)\left[1-\frac{3q}{\gamma_1}+\frac{21q^2}{4\gamma_1^2}\right]+\frac{9q}{8\gamma_1}-\frac{9q^2}{4\gamma_1^2}\right\}, \tag{15}$$

$$v_{1212}(q)=\frac{2\pi e^2}{Sq}\alpha_{1212}\frac{q}{\gamma_0}\left[1-\frac{32q}{5(\gamma_1+\gamma_2)}+\frac{163q^2}{5(\gamma_1+\gamma_2)^2}+\frac{32}{5}\Phi(qd)\left(\frac{q}{\gamma_1+\gamma_2}\right)\left(1-\frac{8q}{\gamma_1+\gamma_2}\right)\right], \quad (16)$$

and

$$v_{1112}(q)=\frac{2\pi e^2}{Sq}\alpha_{1112}\frac{q}{\gamma_0}\left[1+\frac{3\delta}{5}+\frac{3\delta^2}{10}+\frac{\delta^3}{10}-\frac{\delta^6}{80}\times\left(1+\frac{\gamma_2}{\gamma_1}\right)^3[1-\Phi(qd)]\right], \quad (17)$$

where $\Phi(x)=[\varepsilon_s+\varepsilon\coth(x)]/f(x)$, $\gamma_0=m\Lambda_0/\hbar^2$, $\alpha_{1212}=60\gamma_0\gamma_1^3\gamma_2^5/[(\gamma_1+\gamma_2)^7(\gamma_1^2-\gamma_1\gamma_2+\gamma_2^2)]$,

$$\alpha_{1112}=1280\sqrt{3}\gamma_1^{9/2}\gamma_2^{5/2}\gamma_0/[(\gamma_1^2-\gamma_1\gamma_2+\gamma_2^2)^{1/2}(\gamma_1+\gamma_2)\times(3\gamma_1+\gamma_2)^6],$$

and $\delta=1+2\gamma_1/(\gamma_1+\gamma_2)$. For realistic values of d and $E_\perp$, $\alpha_{1212}\sim\alpha_{1112}\sim 10^{-1}$. One estimates that $v_{1111}(q)v_{1212}(q)\gg v_{1112}^2(q)$ in the long wavelength limit. This allows us to disregard $v_{1112}(q)$ in Eq. (5). In such a condition, Eq. (5) splits into two independent equations

$$1-v_{1111}(q)\Pi_{11}^{(0)}(q,\omega)=0, \quad (18)$$

$$1-v_{1212}(q)[\Pi_{12}^{(0)}(q,\omega)+\Pi_{21}^{(0)}(q,\omega)]=0, \quad (19)$$

which give the plasma oscillations over helium films, by considering only virtual transitions from the $n=1$ subband to the first excited $n=2$ subband. Equation (18) describes longitudinal *intrasubband* plasma oscillations whereas Eq. (19) determines the spectrum of transverse *intersubband* oscillations.

Equations (6), (7) and (18), (19) constitute the set of equations which allows us to evaluate the plasmon spectrum in both the nondegenerate and degenerate Q2DES's on a helium film.

A. Longitudinal intrasubband modes

Writing the plasmon frequency as $\omega=\omega_q-i\kappa_q$ we first evaluate the real part ω_q^l of the longitudinal branch. In the limit of $qd\gg 1$, which is attained for $d\to\infty$ at fixed q, we reproduce the results for the nondegenerate Q2DES over bulk helium.[2] The results, however, are quite different in the opposite limit $qd\ll 1$ for thin films and small q. The plasmon spectrum depends, in a crucial way, on the function $\Phi(qd)$ which appears in Eqs. (15) and (16). In this limit $\Phi(qd)$ depends on the relation between ε_s and ε. When both dielectric constants are comparable, even though $\varepsilon_s\gtrsim\varepsilon$, the condition $\varepsilon_s qd/\varepsilon\ll 1$ is fulfilled and $\Phi(qd)$ behaves as

$$\Phi(qd)\simeq\frac{1}{(\varepsilon_s+1)}\left[1+\frac{(\varepsilon_s^2-\varepsilon^2)qd}{\varepsilon(\varepsilon_s+1)}-\frac{(\varepsilon_s+\varepsilon^2)(\varepsilon_s^2-\varepsilon^2)(qd)^2}{\varepsilon^2(\varepsilon_s+1)^2}\right]. \quad (20)$$

In this limit, the longitudinal plasmon frequency can be written as

$$[\omega_q^l]^2\simeq\omega_0^2(q)\left[1+\frac{9}{8}\left(\varepsilon_s-\frac{5}{3}\right)\frac{q}{\gamma_1}+\frac{(\varepsilon_s^2-\varepsilon)qd}{\varepsilon(\varepsilon_s+1)}+\frac{3(\varepsilon_s+1)\tilde{E}q}{4\pi n_s e^2}\right], \quad (21)$$

where we keep, in the brackets, the terms linear in q. Note that the overall structure of ω_q^l, given by Eq. (21), is similar to that of the longitudinal plasma branch for the Q2DES over bulk helium.[2] However, now the frequency $\omega_0^2(q)=4\pi n_s e^2 q/[(\varepsilon_s+1)m]$ instead of $2\pi n_s e^2 q/m$ and the third term corresponds to a finite thickness effect. The additional term $9(\varepsilon_s-5/3)(q/8\gamma_1)$ is positive for $\varepsilon_s>5/3$ whereas it is negative in the case of bulk liquid. The terms in brackets are very small compared with 1 and ω_q^l is nearly given by ω_0.

For $\varepsilon_s qd/\varepsilon\gg 1$, long-wavelength limit ($qd\ll 1$), and strong screening effects ($\varepsilon_s\gg 1$) one obtains

$$\Phi(qd)\simeq\frac{1}{(\varepsilon_s+1)}+\frac{(\varepsilon_s^2-\varepsilon^2)qd}{\varepsilon(\varepsilon_s+1)^2}\left\{1-\frac{\varepsilon_s(\varepsilon_s+\varepsilon^2)qd}{\varepsilon(\varepsilon_s^2-\varepsilon^2)}+\left[\frac{\varepsilon_s(\varepsilon_s+\varepsilon^2)^2}{\varepsilon^2(\varepsilon_s+1)(\varepsilon_s^2-\varepsilon^2)}-\frac{1}{3}\right](qd)^2\right\}. \quad (22)$$

For a metal substrate ($|\varepsilon_s|=\infty$), Eq. (22) reads as

$$\Phi(qd)\simeq\frac{qd}{\varepsilon}\left[1-\frac{qd}{\varepsilon}+\left(\frac{1}{\varepsilon^2}-\frac{1}{3}\right)(qd)^2\right]. \quad (23)$$

The longitudinal mode dispersion for strong screening effects reads as

$$(\omega_q^l)^2\simeq\left[\left(u_0^2+\frac{3\tilde{E}}{m}\right)q^2+\omega_0^2(q)\right]\left\{1-\frac{\varepsilon_s(\varepsilon_s+\varepsilon^2)qd}{\beta\varepsilon(\varepsilon_s^2-\varepsilon^2)}-\frac{3}{\beta}\left[1+\frac{\varepsilon(\varepsilon_s+1)(3\varepsilon_s-4)}{4(\varepsilon_s^2-\varepsilon^2)\gamma_1 d}\right]\frac{q}{\gamma_1}\right\}, \quad (24)$$

where $u_0^2=4\pi\beta(\varepsilon_s^2-\varepsilon^2)e^2 n_s d/m\varepsilon(\varepsilon_s+1)^2$ and $\beta=1+3\varepsilon(\varepsilon_s+1)(3\varepsilon_s-5)/8(\varepsilon_s^2-\varepsilon^2)\gamma_1 d$.

As one can see from Eq. (24) the spectrum is given essentially by two terms. First, an acoustic like mode $\sim q$ and the second one is the usual behavior $\sim q^{1/2}$. By increasing ε_s the last term decreases and vanishes for $|\varepsilon_s|=\infty$. Then for the metal substrate one obtains an acoustic dispersion

$$[\omega_q^l]^2\simeq u^2q^2\left[1-\frac{qd/\varepsilon+3q/\gamma_1+9\varepsilon q/\gamma_1^2 d}{1+9\varepsilon/8\gamma_1 d}\right], \quad (25)$$

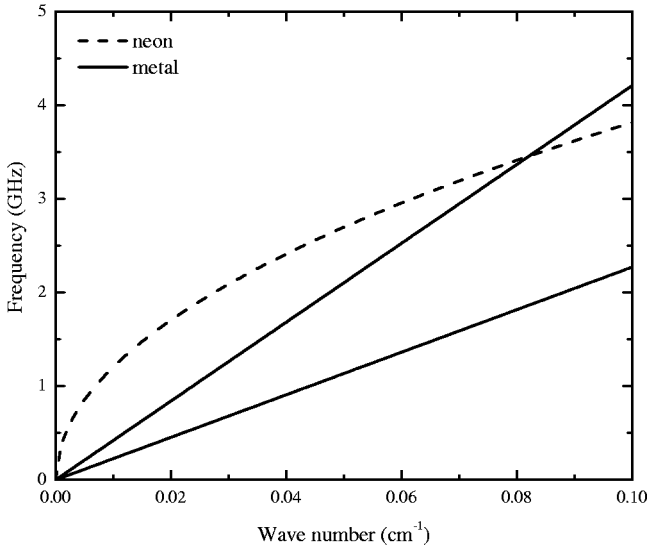

FIG. 1. Longitudinal intrasubband mode frequency for the degenerate Q2DES for a helium film with thickness $d=10^{-6}$ cm (lower solid line) and $d=5\times10^{-6}$ cm (upper solid line) over a metal substrate and neon substrate (dashed line). The frequency scale in the case of a metal is MHz. No marked difference is found in the mode spectrum in the case of neon for these film thicknesses. The relevant parameters are $E_F\cong3$ K, $n_s=10^{11}$ cm^{-2}.

with

$$u^2=\frac{4\pi n_s e^2 d}{\varepsilon m}\left(1+\frac{9\varepsilon}{8\gamma_1 d}\right)+\frac{3\tilde{E}}{m}, \tag{26}$$

which reproduces precisely the results for the longitudinal plasmon in the Q2DES over a metal substrate obtained in both the RPA[13] (except by the effects of the finite width of the electron layer manifested by the term $1+9\varepsilon/8\gamma_1 d$) and in the SCFA.[14,15]

The spectrum for the longitudinal modes of the Q2DES for solid neon and metal substrates is depicted in Fig. 1. We can see that the acoustical behavior is typical for a metal substrate while the usual $q^{1/2}$ dependence is observed for the neon substrate. The dependence on the film thickness is well pronounced in the case of the metal but is negligible for the neon substrate, because in the latter case the screening effects are not strong.

B. Transverse intersubband modes

We consider now the transverse mode whose dispersion relation is defined by Eq. (19). Using Eqs. (7) and (16) one writes the dispersion equation in the long-wavelength limit as

$$[\omega_q^t]^2=\omega_{21}^2+2\omega_{21}\omega_{sh}\left[1-\frac{32\varepsilon_s q}{5(\varepsilon_s-1)(\gamma_1+\gamma_2)}+\frac{32(\varepsilon_s^2-\varepsilon^2)q^2 d}{5\varepsilon(\varepsilon_s+1)^2(\gamma_1+\gamma_2)}+\frac{(1+3\omega_{sh}/2\omega_{21})\tilde{E}q^2}{m\omega_{sh}^2}\right], \tag{27}$$

where $\omega_{sh}=2\pi n_s e^2\alpha_{1212}/\hbar\gamma_0$. Because the term in the brackets depending on q is quite small compared to 1, the dispersion of this mode is negligible. Then screening effects from the substrate slightly modify the transverse plasmon spectrum in contrast with the longitudinal one given by Eqs. (24) and (25). We observe that the transverse mode has the optical gap $[\omega_{21}^2+2\omega_{21}\omega_{sh}]^{1/2}$ at $q=0$ manifesting the effect of depolarization shift relatively to the one-electron spectroscopic frequency ω_{21}. For large enough n_s, ω_{sh} can be comparable to ω_{21}. As an example, for a metal substrate and $d=10^{-6}$ cm, $\omega_{21}=\omega_{sh}\simeq10^{13}$ s^{-1} for $n_s\simeq3\times10^{11}$ cm^{-2}. On the contrary, for smaller n_s, the depolarization shift can be discarded.

Concerning the plasmon damping, the imaginary part κ_q in the degenerate regime is zero within the accuracy of the calculation of the response functions. For the nondegenerate system, κ_q decays exponentially and can be estimated as it was done in Ref. 2.

III. PLASMON SPECTRA FOR THE Q1DES

For the many-body Q1DES laterally confined by a parabolic potential $V(y)=m\omega_{\rm conf}^2 y^2/2$, where $\omega_{\rm conf}=(eE_\perp^*/mR)^{1/2}$ is the confinement frequency, $E_\perp^*$ is the effective holding field, and R is the curvature radius, the dielectric matrix $\epsilon_{nn'mm'}(q_x,\omega)$ is similar to that of the Q2DES given by Eq. (1), but now q_x is the 1D wave number along the channel axis (x).[2] The labels correspond to the electron subbands in the y direction. The plasmon spectra are still defined by Eq. (5) and are reduced, for $\hbar\omega_{\rm conf}\gg T$ ($\hbar\omega_{\rm conf}\simeq0.8$ K for $E_\perp^*=3$ kV/cm and $R=5\times10^{-4}$ cm), to Eqs. (18) and (19) for longitudinal (along the channel) and transverse (across the channel) plasmons.

The exact response functions for the nondegenerate Q1DES were calculated, within the RPA, for arbitrary subband index and q_x.[2] However, when we consider film effects, one cannot exclude the possibility that the quantum regime can be achieved at high linear densities n_l. For instance, the 1D Fermi energy $E_F^{(1D)}=\pi^2\hbar^2 n_l^2/8m\simeq10^{-1}$ K, for $n_l=10^5$ cm^{-1}. Note that n_l is the inverse of the mean interparticle distance a along the channel—i.e., $n_l^{-1}\simeq a$. The calculation of the response functions is rather simple for $T=0$. The results are[34]

$$\mathrm{Re}\,\Pi_{11}^0(q_x,\omega)=\frac{N}{2\hbar v_F q_x}\ln\left[\frac{\omega^2-(v_F q_x-\hbar q_x^2/2m)^2}{\omega^2-(v_F q_x+\hbar q_x^2/2m)^2}\right], \tag{28}$$

$$\mathrm{Re}[\Pi_{12}^0(q_x,\omega)+\Pi_{21}^0(q_x,\omega)]=\frac{N}{2\hbar v_F q_x}\ln\left[\frac{\omega^2-(\omega_0-v_F q_x+\hbar q_x^2/2m)^2}{\omega^2-(\omega_0+v_F q_x+\hbar q_x^2/2m)^2}\right], \tag{29}$$

where $v_F^{(1D)}=\pi\hbar n_l/(2m)$ is the 1D Fermi velocity. The imaginary part of the response functions is zero.

We point out that in the long-wavelength limit the real part of the response functions is given by similar expressions

for both nondegenerate and degenerate regimes and are the same as Eqs. (6) and (7), but q_x replaces q, $\omega_{21}=\omega_{\rm conf}$, and $\tilde{E}=(2/3)E_F$ in the degenerate limit. As for the Q2DES, the imaginary part of the response functions is nonzero only for the nondegenerate Q1DES and is exponentially small in the long wavelength limit.

The Q1D Coulomb potential is calculated from Poisson's equation and given by

$$v(q_x)=\frac{2e^{*2}}{L_x}[K_0(|q_x||y'-y|) - \sigma K_0(|q_x|\sqrt{(y'-y)^2+4d^2})], \tag{30}$$

where L_x is the system size in the x direction, $\sigma=2\varepsilon(\varepsilon_s-\varepsilon)/[(1+\varepsilon)(\varepsilon_s+\varepsilon)]$, and $K_0(x)$ is the modified Bessel function. To calculate the matrix element we employ the usual harmonic oscillator functions.[35,36] It is not possible to evaluate the matrix elements for arbitrary subband indices. However, in the two-subband model, we can use the explicit form of wave functions for the lowest ($n=1$) and first excited ($n=2$) subbands to calculate $v_{1111}(q_x)$ and $v_{1212}(q_x)$. One can easily show that the matrix element $v_{1112}(q_x)=0$ in Q1DES not only for bulk helium[36] but also for a helium film.

A. Longitudinal intrasubband modes

The diagonal matrix element is

$$v_{1111}(q_x)=\frac{e^{*2}}{L_x}\left[e^{q_x^2l^2/4}K_0(q_x^2l^2/4)-\left(\frac{8\sigma^2}{\pi}\right)^{1/2}\int_0^\infty e^{-x^2/2} \times K_0(|q_xl|\sqrt{x^2+4d^2/l^2})dx\right], \tag{31}$$

where $l=(\hbar/m\omega_{\rm conf})^{1/2}$ and we restrict ourselves to $n=1$ in the series of Eq. (10).

In the most interesting limit $|q_xl|\ll 1$, the asymptotic expressions depend strongly on the relation between l and d. Note that l decreases slowly as a function of $E_\perp$ and is $\simeq 3\times10^{-6}\ll R\sim10^{-4}$–$10^{-3}$ cm for $E_\perp=3$ kV/cm.

1. Thick films

If $d>l$ (relatively thick films), one has

$$v_{1111}(q_x)=\frac{e^{*2}}{L_x}\{\exp(q_x^2l^2/4)K_0(q_x^2l^2/4)-2\sigma K_0(2|q_xd|)\}, \tag{32}$$

and two limiting cases can be analyzed.

(i) For $|q_xd|\gg 1$, $K_0(2|q_xd|)\to 0$ and we reproduce the result for the Q1DES over bulk helium:[36]

$$v_{1111}(q_x)\simeq\frac{2e^{*2}}{L_x}\ln\frac{1}{|q_xl|}. \tag{33}$$

From Eq. (33) the following dispersion law for the longitudinal plasmon, calculated using Eq. (18), is given by

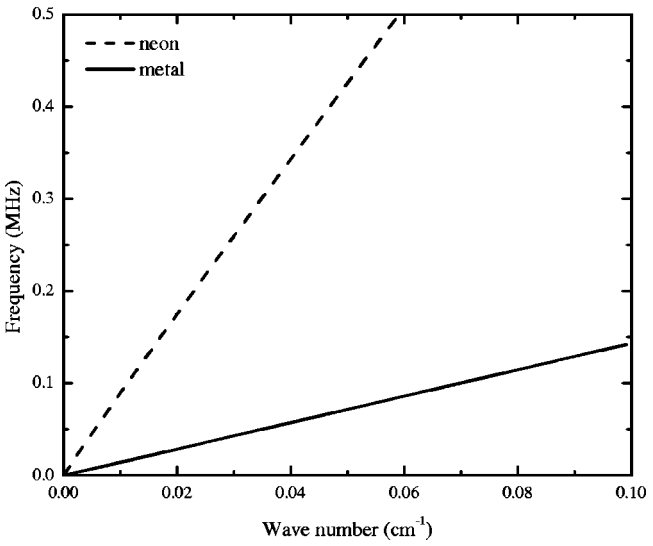

FIG. 2. Longitudinal mode frequency for the degenerate Q1DES for $d=5\times10^{-6}$ cm over a metal substrate (solid line) and neon substrate (dashed line). The frequency scale in the case of a metal is kHz and $E_F=0.1$ K and $a\simeq n_l^{-1}=10^{-4}$ cm.

$$\omega_l^2(q_x)=\frac{2e^{*2}}{ma}q_x^2\ln\frac{1}{|q_xl|}+\frac{3\tilde{E}q_x^2}{m}. \tag{34}$$

The first term of Eq. (34) is the well-known result for the longitudinal mode[21] and the second term is a small correction.

(ii) However, in the more interesting limits $|q_xl|\ll 1$ and $|q_xd|\ll 1$ we obtain

$$v_{1111}(q_x)=\frac{2e^{*2}}{L_x}\ln\frac{|q_xd|^\sigma}{|q_xl|} \tag{35}$$

and thereby the plasmon spectrum

$$\omega_l^2(q_x)=\frac{2e^{*2}}{ma}q_x^2\ln\frac{|q_xd|^\sigma}{|q_xl|}+\frac{3\tilde{E}q_x^2}{m}. \tag{36}$$

The contribution of the second term is small in comparison with the first term for any reasonable parameters. For a metal substrate ($\varepsilon_s=\infty$, and $\sigma\simeq 1$), $v_{1111}(q_x)\simeq(2e^{*2}/L_x)\ln(d/l)$, and the dispersion relation is purely acoustical $\omega_l(q_x)=c_{lq}q_x$, with $c_{lq}^2=(2e^{*2}/ma)\ln(d/l)+3\tilde{E}/m$. A typical value is $c_{lq}\simeq 2.4\times10^6$ cm/s for $d/l=3$ (hereafter we take $a=10^{-4}$ cm), which is nearly 3–4 times smaller than the sound velocity in Eq. (34) for $|q_xl|=10^{-5}$.

In Fig. 2, we show the longitudinal modes of the Q1DES for metal and neon substrates obtained from Eq. (36). The acoustical mode behavior is seen in the case of both substrates.

2. Thin films

When $d<l$ and for asymptotic limits of $|q_xl|\ll 1$, $|q_xd|\ll 1$, we obtain

$$v_{1111}(q_x)=\frac{2e^{*2}}{L_x}\left[(1-\sigma)\ln\frac{1}{|q_xl|}+(2\pi)^{1/2}\sigma(d/l)\right]. \tag{37}$$

Values of σ depend strongly on the substrate dielectric constant and $\sigma \simeq 1.03$ at $|\varepsilon_s| \to \infty$. It means that, for a metal substrate, the second term in Eq. (37) should be larger than the first term. In this case one can disregard the logarithmic term when $d/l \gtrsim 0.2$ for $|q_x l| \sim 10^{-5}$. In such a condition, $v_{1111}(q_x) \simeq (2^{3/2}\pi^{1/2}e^{*2})(d/L_x l)$. The longitudinal mode is still acoustical, but the sound velocity is now $c_{lq}^2 = (2^{3/2}\pi^{1/2} d e^{*2})/mal + 3\tilde{E}/m \simeq 2.1 \times 10^6$ cm/s.

B. Transverse intersubband modes

In contrast to the Q2DES, both longitudinal and transverse plasmons of the Q1DES are connected with the quantization requirement along the y direction. Therefore one should expect strong screening effects from the substrate not only on $v_{1111}(q_x)$ but also on $v_{1212}(q_x)$. Indeed the general expression for $v_{1212}(q_x)$ can be written as

$$v_{1212}(q_x) = \frac{e^{*2}}{L_x}\left\{ e^{q_x^2 l^2/4}\left[K_0(q_x^2 l^2/4) - \frac{\pi^{1/2}}{2^{1/2}|q_x l|} W_{-1,0}(q_x^2 l^2/2)\right] - \left(\frac{8\sigma^2}{\pi}\right)^{1/2} \times \int_0^\infty e^{-x^2/2}(1-x^2) \times K_0(|q_x l|\sqrt{x^2 + 4d^2/l^2})\,dx \right\}, \tag{38}$$

where $W_{a,b}(x)$ is the Whittaker function.

1. Thick films

Evaluating the asymptotic expression for $d > l$ in Eq. (38), when $|q_x d| \gg 1$ and $|q_x l| \ll 1$, we arrive at the result for the Q1DES over bulk helium, $v_{1212}(q_x) = (e^{*2}/L_x)[1 - (q_x^2 l^2/2)\ln|q_x l|^{-1}]$, which leads to the transverse plasma spectrum branch[2]

$$\omega_t^2(q_x) = \omega_0^2 - \frac{e^{*2} q_x^2}{ma}\ln\frac{1}{|q_x l|} + 2\omega_0\omega_{sh}^{1D} \times \left\{ 1 + \left[\frac{(1 + 3\omega_{sh}^{1D}/2\omega_0)\tilde{E}}{m(\omega_{sh}^{1D})^2} + \frac{(1 + \omega_{sh}^{1D}/\omega_0)\hbar}{2m\omega_{sh}^{1D}} q_x^2 \right] \right\}, \tag{39}$$

with the depolarization shift frequency $\omega_{sh}^{1D} = e^{*2}/\hbar a$.

If $|q_x l| \ll 1$ and $|q_x d| \ll 1$, the transverse mode is still described by Eq. (39), but now $\omega_{sh}^{1D} = [1 - \sigma l^2/4d^2]e^{*2}/\hbar a$, shifting slightly to lower frequencies in comparison with the bulk case.

2. Thin films

For $d < l$ and $|q_x l| \ll 1$, $|q_x d| \ll 1$ the transverse mode is written as

$$\omega_t^2(q_x) \simeq \omega_0^2 - (1-\sigma)\frac{e^{*2} q_x^2}{ma}\ln\frac{1}{|q_x l|} + 2\omega_0\omega_{sh}^{1D} \times \left\{ 1 + \left[\frac{(1 + 3\omega_{sh}^{1D}/2\omega_0)\tilde{E}}{m(\omega_{sh}^{1D})^2} + \frac{(1 + \omega_{sh}^{1D}/\omega_0)\hbar}{2m\omega_{sh}^{1D}} \right] q_x^2 \right\}, \tag{40}$$

where $\omega_{sh}^{1D} = (e^{*2}/\hbar a)\{1 - \sigma[1 - \sqrt{2\pi}(d/l)]\}$. For a metal, $\omega_{sh}^{1D} = (2\pi)^{1/2}[e^{*2} d/\hbar a l]$. We estimate $\omega_{sh}^{1D} \simeq 1.8 \times 10^{12}$ s^{-1} for $d/l = 1/3$, which should be compared with $\omega_{\rm conf} \sim 10^{11}$ s^{-1}.

IV. CONCLUDING REMARKS

We have studied the collective modes of Q2DES and Q1DES floating over a cryogenic film deposited on a solid substrate. We have shown that screening effects from the substrate lead to essential modification of the plasmon spectrum in comparison with the bulk results. Special attention was given to the case of large ε_s where the liquid-phase region in the plane (n_s, T) of the Q2DES is considerably enhanced for small d.[12] The dispersion relations for longitudinal intrasubband and transverse intersubband plasmons were calculated in both the nondegenerate and degenerate regimes. The Q1DES itinerant phase was also considered for thick and thin films in the limit of long wavelength. We found in both ES's a Goldstone mode spectrum for longitudinal plasmons and an optical transverse mode with negligible dispersion. The value of the mode gap is nearly given by the spectroscopic transition frequency between the ground and first excited subbands. The mode frequency dependence on the electron density was also estimated for a certain range of electron densities.

ACKNOWLEDGMENTS

This work was supported in part by grants from Fundação de Amparo à Pesquisa do Estado de São Paulo (FAPESP) and the Conselho Nacional de Desenvolvimento Científico e Tecnológico (CNPq). We are grateful to Dr. J.M. Villas-Bôas for discussion of the numerical results.

[1] See the review papers in *Two-dimensional Electron Systems in Helium and Other Substrates*, edited by E. Y. Andrei (Kluwer, Dordrecht, 1997).
[2] S.S. Sokolov and N. Studart, J. Phys.: Condens. Matter **12**, 9563 (2000).
[3] L.P. Gorkov and D.M. Chernikova, Pis. Zh. Eksp. Teor. Fiz. **18**, 119 (1973) [Sov. Phys. JETP **18**, 68 (1973)].
[4] M. Wanner and P. Leiderer, Phys. Rev. Lett. **42**, 315 (1979).
[5] A.J. Dahm, in Ref. 1 and references therein.
[6] H. Ikezi and P.M. Platzman, Phys. Rev. B **23**, 1145 (1981).

[7] V.V. Tatarskii, N.I. Shikina, and V.B. Shikin, Zh. Éksp. Teor. Fiz. **82**, 747 (1982) [Sov. Phys. JETP **55**, 444 (1982)].
[8] G. Mistura, T. Günzler, S. Neser, and P. Leiderer, Phys. Rev. B **56**, 8360 (1997).
[9] H. Etz, W. Gombert, W. Idstein, and P. Leiderer, Phys. Rev. Lett. **53**, 2567 (1984).
[10] X.L. Hu and A.J. Dahm, Phys. Rev. B **42**, 2010 (1990).
[11] T. Günzler, B. Bitnar, G. Mistura, S. Neser, and P. Leiderer, Surf. Sci. **341/342**, 831 (1996).
[12] F.M. Peeters and P.M. Platzman, Phys. Rev. Lett. **50**, 2021 (1983).
[13] Yu.P. Monarkha, Fiz. Nizk. Temp. **3**, 1459 (1977) [Sov. J. Low Temp. Phys. **3**, 702 (1977)].
[14] J.P. Rino, N. Studart, and O. Hipólito, Phys. Rev. B **29**, 2584 (1984).
[15] U. de Freitas, L.C. Ioriatti, and N. Studart, J. Phys. C **20**, 5983 (1987).
[16] S.S. Sokolov and N. Studart, Phys. Rev. B **66**, 075424 (2002).
[17] V.B. Shikin and Yu.P. Monarkha, J. Low Temp. Phys. **16**, 193 (1974).
[18] P. Glasson, V. Dotsenko, P. Fozooni, M.J. Lea, W. Bailey, G. Papageorgiou, S.E. Andersen, and A. Kristensen, Phys. Rev. Lett. **87**, 176802 (2001).
[19] S.P. Gladchenko, V.A. Nikolaenko, Yu.Z. Kovdrya, and S.S. Sokolov, Fiz. Nizk. Temp. **27**, 3 (2000) [Low Temp. Phys. **27**, 3 (2000)].
[20] R.J.F. van Haren, G. Acres, P. Fozooni, A. Kristensen, M.J. Lea, P.J. Richardson, A.M.C. Valkering, and R.W. van der Heijden, Physica B **249-251**, 656 (1998).
[21] S.S. Sokolov and N. Studart, Phys. Rev. B **57**, R704 (1998).
[22] S.S. Sokolov and N. Studart, Phys. Rev. B **60**, 15 562 (1999).
[23] B. Vinter, Phys. Rev. B **15**, 3947 (1977).
[24] S. Das Sarma, Phys. Rev. B **29**, 2334 (1984).
[25] P.M. Platzman and N. Tzoar, Phys. Rev. B **13**, 1459 (1976).
[26] N. Studart and O. Hipólito, Phys. Rev. A **19**, 1790 (1979).
[27] F. Stern, Phys. Rev. Lett. **18**, 546 (1967).
[28] A.L. Fetter and J.D. Walecka, *Quantum Theory of Many-Particle Systems* (McGraw-Hill, New York, 1971).
[29] W.R. Smythe, *Static and Dynamic Electricity* (McGraw-Hill, New York, 1950).
[30] S.S. Sokolov and N. Studart, Phys. Rev. B **67**, 132510 (2003).
[31] Yu.P. Monarkha, S.S. Sokolov, and V.B. Shikin, Solid State Commun. **38**, 611 (1981).
[32] S.S. Sokolov, Fiz. Nizk. Temp. **11**, 875 (1085) [Sov. J. Low Temp. Phys. **11**, 481 (1985)].
[33] S.S. Sokolov, J.P. Rino, and N. Studart, Phys. Rev. B **55**, 14 473 (1997).
[34] Q. Li and S. Das Sarma, Phys. Rev. B **40**, 5860 (1989).
[35] N. Studart and S.S. Sokolov, in Ref. 1.
[36] G.Y. Hu and R.F. O'Connell, Phys. Rev. B **42**, 1290 (1990).